Lifetime of excited electronic states at surfaces: Comparison between the alkali/Cu(111) systems

A. G. Borisov and J. P. Gauyacq
Laboratoire des Collisions Atomiques et Moléculaires, Unité Mixte de Recherche CNRS-Université Paris Sud UMR 8625, Bâtiment 351, Université Paris-Sud, 91405 Orsay Cedex, France

E. V. Chulkov, V. M. Silkin, and P. M. Echenique
Departamento de Física de Materiales, Facultad de Ciencias Químicas, Universidad del País Vasco/Euskal Herrriko Unibertsitatea, Donostia International Physics Center (DIPC) y Centro Mixto CSIC-UPV/EHU, Apartado 1072, 20018 San Sebastian Donostia, Spain
(Received 15 February 2002; published 21 June 2002)

Time-resolved two-photon photoemission of alkali adsorbates on noble-metal surfaces revealed the existence of very long-lived excited electronic states. The present work is devoted to the study of the lifetime of electronically excited states in the alkali/Cu(111) systems. The cases of Na, K, Rb, and Cs are investigated. The decay by one-electron transitions (resonant charge transfer) and by multielectron interactions (inelastic electron-electron scattering in the bulk and at surface) is evaluated in a joint wave-packet propagation and many-body metal response approach. The origin of the stabilization of the excited states is stressed and the difference between the decay rates of the various alkalis is discussed and shown to be connected to the alkali polarizability. The present theoretical results are compared with the available experimental data.

DOI: 10.1103/PhysRevB.65.235434 PACS number(s): 73.20.Hb, 34.70.+e, 73.40.Gk, 82.65.+r

I. INTRODUCTION

Recently, the experimental observation by time-resolved two-photon photoemission (TR-2PPE) of extremely long-lived excited electronic states in the Cs/Cu(111) system attracted a lot of attention in the field of excited-state dynamics.[1–4] This interest was aroused both because these results were unexpected and because of their potentially important consequences for surface reaction mechanisms. Indeed, many surface reaction mechanisms involve the transient formation of electronically excited states, the relaxation of which can lead to a variety of processes: electron to nucleus energy transfer, desorption, fragmentation of adsorbates, chemical reactions.[5] However, these excited states can also relax by giving away their excitation energy to the substrate electrons, resulting in the quenching of the reaction mechanism. In the case of an atomic or molecular adsorbate on a metallic substrate, the decay of an excited state by electron transfer between the adsorbate and the substrate is usually thought to be extremely fast. Indeed, theoretical studies of alkali atoms in front of free-electron (jellium) metals lead to transient state lifetimes in the 0.5-fs range.[6–8] Such a short lifetime of the transient state considerably limits the efficiency of an excited-state-mediated process. Thus, the understanding of the experimental observations of long-lived adsorbate states could open the way to the design of efficient reaction mechanisms, compared to what is known for free-electron metal surfaces.

The excited-state lifetimes found in the alkalis on Cu(111) and Cu(100) systems by TR-2PPE experiments are much longer than what was computed in the case of alkalis on free-electron metal systems: an excited electronic state with a lifetime of a few tens of femtoseconds was found in the Cs/Cu(111) system[1–4] at low coverage. This excited state corresponds to the transient capture of a metal electron by the ionic Cs adsorbate. The long lifetime was shown to allow a significant motion of the Cs adsorbate during the lifetime of the excited state; this leads both to important modifications of the time dependence of the TR-2PPE signal[4,9,10] and to the existence of a photoinduced Cs desorption process.[4] Long lifetimes, although shorter, were also reported for other alkali adsorbates on noble metals such as Cs/Cu(100), Cs/Ag(111), and Rb/Cu(111).[1–3,9] However, no very long lived state was observed in the case of Na adsorbate on Cu(111) and Cu(100), where lifetimes of 1.6 and 4 fs, respectively, were reported.[2,9]

In the alkali/metal systems, the excited state can decay by resonant tunneling of the excited electron from the alkali adsorbate to the substrate, i.e., by transitions from the atomic state to a metal state of the same energy. This process is usually termed resonant charge transfer (RCT). In the case of a free-electron metal surface, electron tunneling occurs preferentially along the surface normal where the transparency of the barrier separating the adsorbate and the metal is the largest. The very long lived state in the Cs/Cu(111) has been attributed to a peculiarity of the Cu electronic band structure:[11,12] a projected band gap that forbids the penetration of electrons into the metal along the surface normal in a certain energy range. It was shown that associated with the polarization of the Cs electronic cloud, this band gap leads to an efficient blocking of the RCT process. In such a situation, other decay channels can play a role. In particular, the decay of the excited electron by inelastic interactions with the substrate electrons can start to play a role. Usually, this multielectron process is weaker than the RCT one-electron process; however, in the present case, the weakness of the RCT process makes the multielectron process visible. Because of these features, the long-lived excited state in Cs/Cu(111) looks very much like a localized equivalent of the image potential states.[13–16] It has been shown that for the Cs/Cu(111) and Cs/Cu(100) systems, the multielectron interaction decay together with the RCT decay accounts for the experimental observations and, in particular, for the difference between the two Cu surfaces.[17]

An excited electronic state can also decay via the excitation of bulk or surface phonons. The corresponding contribution has been computed in the case of surface and image states on Cu(111) and Ag(111).[18] Comparison between the decay rates induced by electron-phonon interactions in the surface and image state case [7 meV and of the order of 1 meV, respectively, at 0 K (Ref. 18)] shows that this process is weak for states localized far from the surface. In the case of the alkali-localized states in Alk/Cu(111), the resonant electronic cloud is repelled from the surface [see below and in (Refs. 11 and 12)], weakening the electron-phonon interaction. In the present work, we did not evaluate this contribution to the state decay.

It is also worth mentioning that the RCT process plays also a very important role in the collisional charge transfer between ions and metal surfaces (see, e.g., a review in Ref. 19) and indeed, the RCT blocking due to a projected band gap can strongly influence the charge state of reflected particles in an ion-surface collision. Such effects have been predicted and their various aspects have been confirmed experimentally:[20–23] blocking of the RCT, interaction time dependence of the projected band gap effect, and the role of the 2D surface states.

Although many atoms or molecules interacting with a noble-metal surface can lead to the situation of an atomic (molecular) level degenerate with a projected band gap, it appeared that not all of these systems exhibit a very long lived excited state. As an example, the $2\pi^*$ resonance of CO adsorbed on Cu is short-lived.[12,24–28] Various effects play a role to enhance or decrease the RCT blocking due to the projected band gap: polarization of the excited state, role of the surface and image states, symmetry of the level, charge state of the level (see discussion in Ref. 12). Various systems have been investigated theoretically,[11,12,20,27,29] leading to the conclusion that neutral polarizable adsorbates were the best systems for looking for long-lived states. Alkalis are thus good candidates for unusually long lifetimes.

In the present work, we theoretically study the case of various alkalis, Na, K, Rb, and Cs, adsorbed on Cu(111) surfaces. All lead to adsorbate states degenerate with the Cu(111) projected band gap and can thus be expected to exhibit a RCT blocking effect. We determine the decay rate of the levels both by one-electron and by multielectron interactions, with the aim of understanding the differences between the various alkalis. This work complements our earlier work on Cs/Cu systems,[17] where we discussed the differences between the various Cu surfaces.

II. METHODS

The calculation of the excited-state characteristics (energy and lifetime) of the alkali/Cu(111) systems has been performed in the case of a single alkali adsorbate on the Cu(111) surface. The present results should then correspond to the case of low alkali coverage on the surface. These calculations have been performed for a range of fixed distances Z between the adsorbate and the substrate. For long-lived states such as those studied here, one can expect the adsorbate to move with respect to the substrate during the state lifetime. However, even if this results in profound changes in the experimental observations (see in Refs. 4, 9, and 10), this does not play a role in the present study of the differences between the various alkali excited-state lifetimes.

The present work is performed in two successive steps: (i) a wave-packet propagation (WPP) study of the alkali/Cu(111) system, which yields the one-electron decay rate and the wave function of the resonant state, and (ii) the parameter-free calculation of the inelastic electron-electron decay rate using the wave function determined in step (i). (Atomic units are used, i.e., $\hbar = e^2 = m = 1$, except otherwise stated.)

A. Wave-packet propagation study

The WPP approach has already been presented in detail earlier,[21,29] and we only give here a short presentation of the specificity of the present study.

Since the RCT process is a one-electron process, we can restrict its study to that of an electron moving in a potential created by the surface and the adsorbate core. The WPP procedure consists in studying the time evolution of a wave packet $\Psi(t)$ describing the active electron in the alkali/Cu system. The analysis of the time evolution of $\Psi(t)$ allows the extraction of the energy and width of the quasistationary states of the system and the determination of the corresponding wave functions. The one-electron Hamiltonian is given by

$$H = T + V_{\text{core}} + V_{\text{Cu}} + \Delta V_{\text{Cu}} = T + U, \tag{1}$$

where T is the electron kinetic energy, V_{core} represents the interaction between the electron and the alkali adsorbate core, V_{Cu} represents the electron interaction between the electron and the Cu(111) surface, and ΔV_{Cu} represents the change of V_{Cu} due to the presence of the adsorbate core.

The interaction of the electron with the ionic alkali core is described by a nonlocal pseudopotential, derived from the pseudopotentials determined by Bardsley[30] for the alkalis. The potentials in Ref. 30 being l dependent [$U_l(r)$, where r is the electron-alkali center distance], we could not use them directly in the present wave-packet propagation scheme. We transformed them into a nonlocal pseudopotential of the Kleinman-Bylander[31,32] form:

$$V_{\text{core}} = U_0(r) + \sum_{l=1,2} \frac{|\Delta U_l \phi_l\rangle\langle \phi_l \Delta U_l|}{\langle \phi_l|\Delta U_l|\phi_l\rangle}, \tag{2}$$

where $\Delta U_l(r) = U_l(r) - U_0(r)$. ϕ_l are the wave functions for the free alkali atom, corresponding to the lowest states of p and d symmetry, associated with the pseudopotential from Ref. 30. The various potentials have been saturated and taken constant below a distance of 1 a_0, to avoid the potential divergences in the WPP. These pseudopotentials reproduce quite well the excited-state spectra of the alkali atoms. Typically, the excited-state energies differ from those obtained with Bardsley pseudopotentials by less than 5 meV.

The V_{Cu} interaction is taken as a local potential adjusted from an *ab initio* density-functional theory study;[33] it only considers the modulation of the potential along the surface

normal and assumes a free-electron motion parallel to the surface. It joins an image charge attraction potential in vacuum to a potential oscillating with the (111) spatial frequency inside bulk Cu. The V_{Cu} potential reproduces the Cu(111) features that are important for the present RCT study: position of the L-band gap (between -5.83 and -0.69 eV with respect to vacuum), position of the surface state (5.27 eV below vacuum) and of the first image state (0.82 eV below vacuum). Since the adsorbate core is ionic, it perturbs the Cu surface and the corresponding change in the electron-Cu interaction potential ΔV_{Cu} is described by an image charge interaction.

The wave function $\Psi(t)$ of the active electron is discretized on a two-dimensional (2D) mesh of points in cylindrical coordinates (z,ρ). The z axis is the symmetry axis of the problem, i.e., the axis normal to the surface and going through the adsorbate center. Only states of σ symmetry are considered here, corresponding to the lowest transient state of the problem. The time-dependent Schrödinger equation with the Hamiltonian (1) is directly solved using the split-propagation technique:[34,35]

$$\Psi(t+dt)=e^{-i\Delta t(T+U)}\Psi(t) \\ =e^{-i(\Delta t/2)U}e^{-i\Delta tT}e^{-i(\Delta t/2)U}\Psi(t). \qquad (3)$$

A finite difference scheme together with the Cayley transform is used to represent the z and ρ parts of the kinetic-energy operator in Eq. (3). To suppress artificial reflections of the wave packet, a complex absorbing potential[36–38] is introduced at the grid boundaries. The initial state $\Psi(t=0)$ of the propagation is taken equal to the wave function ϕ_0 of the lowest s state of the alkali in the free atom. The wave-packet survival amplitude $A(t)=\langle\Psi(t=0)|\Psi(t)\rangle$ as a function of time is then analyzed as the sum of a few complex exponential functions,[21] yielding the quasistationary state energy and width. These widths are equal to the decay rate of the quasistationary state by a one-electron interaction (RCT process) and are termed Γ_{RCT} below.

Extracting the resonance wave function Ψ_R to be used in the computation of the multielectron decay rate is more elaborate. Indeed, since the resonance state in the case of a finite alkali-Cu distance is different from the free-atom state, the wave packet $\Psi(t)$ described above contains terms other than the resonance wave function. One could first think of the simplest procedure consisting in removing these nonresonant components by simply letting the propagation run for a long time, while renormalizing the wave packet from time to time. For late times, only the long-lived component in the wave packet, i.e., the resonant component, will survive. Unfortunately, the low-energy (small $k_{\parallel}$, electron momentum parallel to the surface) states of the surface and image state continuum that are present in the initial wave packet significantly contribute to $\Psi(t)$ over a very long time. This makes this simple resonant wave-function extraction inefficient. To extract Ψ_R, we rather used the following procedure: (i) we introduce an additional absorbing potential inside the bulk, extending from the image plane position and (ii) we artificially shift down the Cu projected band gap. The absorbing potential close to the surface leads to a fast decay of the surface state component, while being much less efficient on the adsorbate localized transient state and on the image state components. The downshift of the band gap brings the image state in resonance with 3D propagating bulk states and thus leads to its very fast decay. In the course of the propagation, the additional absorbing potential is adiabatically reduced to zero and the band gap is also adiabatically moved back to its usual position, given by the potential.[33] Extracting the resonance wave function Ψ_R with the above procedure requires a typical propagation time of around 4000 a.u. (around 100 fs). Recently, we tested another Ψ_R extraction procedure, which turns out to be more efficient. It consists in extracting the component at the resonance energy E_0 from the wave packet $\Psi(t)$. Ψ_R is defined as

$$\Psi_R=\int_0^T e^{iE_0t}\Psi(t)dt. \qquad (4)$$

This procedure requires two wave-packet time propagations: in the first one, the transient state energy E_0 is obtained and in the second one the integral (4) is computed. The latter is best implemented inside the wave-packet propagation, the integral (4) being performed along with the wave-packet propagation:

$$\Psi_R(t+dt)=\Psi_R(t)+dte^{iE_0(t+dt)}\Psi(t+dt). \qquad (5)$$

The propagation time required for getting Ψ_R in that case depends on the energy difference between the various states. It typically amounts to 2000 a.u. and leads to a much faster convergence than the other methods.

B. Decay by multielectron interactions

The inelastic contribution to the decay rate Γ_{ee} of an excited electron in the alkali/Cu(111) system is calculated as the projection of the imaginary part of the quasiparticle self-energy, $\mathrm{Im}(\Sigma(\vec{r},\vec{r}\,';E_0))$, onto the quantum state of interest (see, for instance, Ref. 39 and references therein):

$$\Gamma_{\mathrm{ee}}=-2\int\int d\vec{r}\,d\vec{r}\,'\Psi_R^*(\vec{r})\mathrm{Im}(\Sigma(\vec{r},\vec{r}\,';E_0))\Psi_R(\vec{r}\,'), \qquad (6)$$

where E_0 is the energy of the excited state. Ψ_R is the excited-state wave function. In the present study, Ψ_R is the resonance wave function determined in the preceding section. It thus includes the perturbations of the alkali-localized states induced by the vicinity of the surface and is very different from a free-atom wave function [see Figs. 3(a) and 3(b) for the Na and Cs cases].

A system with a single adatom on the metal surface is not translation invariant since it combines an extended system (semi-infinite substrate characterized by 2D translational symmetry) and a very local system (0D adsorbate localized state). The accurate calculation of the self-energy for such a system is an extremely complicated problem of many-body theory. Therefore, in practical calculations, we approximate the self-energy of the alkali/Cu(111) system by that evaluated for a clean metal substrate, Cu(111). We calculate the

self-energy of the substrate by using the so-called GW approximation,[40] which represents the first term in the series expansion of Σ in terms of the screened Coulomb interaction. Replacing the full one-electron Green function by the noninteracting Green function, we obtain the following contribution to the inelastic decay rate of a state at energy E_0:

$$\Gamma_{ee} = -2 \sum_{E_{n,\vec{k}}}^{E_0 \geqslant E_{n,\vec{k}} \geqslant E_F} \int\int d\vec{r} d\vec{r}\,' \Psi_R^*(\vec{r}) \psi_{n,\vec{k}}(\vec{r}) \times \mathrm{Im}(W(\vec{r},\vec{r}\,';E_0 - E_{n,\vec{k}})) \Psi_R(\vec{r}\,') \psi_{n,\vec{k}}^*(\vec{r}\,'), \quad (7)$$

where the sum is extended over all final states $\psi_{n,\vec{k}}(\vec{r})$ with energy $E_{n,\vec{k}}$, n labels both bulk and surface electron bands and $\vec{k}$ is the 2D momentum. To avoid the very long computing times involved in three-dimensional calculations, we assume that the charge density and one-electron potential vary only in the z direction perpendicular to the surface and are constant in the (x,y) plane parallel to the surface. In this one-dimensional model the wave functions are of the form

$$\psi_{n,\vec{k}}(\vec{r}) = \frac{l}{L} e^{i\vec{k}\vec{\rho}} \varphi_n(z), \quad (8)$$

where L is a normalization constant and the one-electron energies are

$$E_{n,\vec{k}} = E_n + \frac{\vec{k}^2}{2m_n^*}. \quad (9)$$

$\varphi_n(z)$ and E_n are the eigenfunctions and eigenenergies of the one-dimensional model potential.[33] They describe the electron motion perpendicular to the surface. We also introduce effective masses m_n^* to approximately account for the surface corrugation parallel to the surface. Finally the two-dimensional Fourier-transform of $\mathrm{Im}(\Sigma)$ is obtained as

$$\mathrm{Im}(\Sigma(z,z';\vec{q};E_0)) = \frac{1}{(2\pi)^2} \sum_{E_n}^{E_0 \geqslant E_n \geqslant E_F} \varphi_n^*(z') \varphi_n(z) \times \int \mathrm{Im}\left[W\left(z,z';\vec{q}-\vec{k};E_0 - E_n + \frac{\vec{q}^2}{2m_0^*} - \frac{\vec{k}^2}{2m_n^*} \right) \right] d\vec{k}. \quad (10)$$

The details of the calculation of the wave functions $\varphi_n(z)$ and of the imaginary part of the screened Coulomb interaction $\mathrm{Im}(W)$ are given in Refs. 39 and 41. From the Fourier transforms $\mathrm{Im}(\Sigma(z,z';\vec{q};E_0))$, we obtain $\mathrm{Im}(\Sigma(\vec{r},\vec{r}\,';E_0))$ and then the decay rate Γ_{ee} of the excited state of the alkali/Cu(111) system is computed using cylindrical coordinates.

C. Total decay rate

The total decay rate Γ_T inverse of the quasistationary state lifetime τ is obtained by summing the two contributions, one-electron and multielectron decay rates:

$$\Gamma_T = \frac{1}{\tau} = \Gamma_{\mathrm{RCT}} + \Gamma_{\mathrm{ee}}.$$

This implicitly assumes that the two decay channels of the quasistationary state can be treated independently, i.e., that the RCT decay is not perturbed by the existence of the multielectron decay inside the metal. The validity of this assumption for long-lived adsorbate localized states has been assessed in Ref. 17 by performing model studies in which the effect of the multielectron decay is described by a local imaginary potential, similarly to low-energy electron diffraction (LEED) studies.[42]

One can stress that the two decay channels of the quasistationary states lead to very different final states. In the RCT case, the decay populates Cu states with the same energy as the quasistationary state and with a very large $k_\parallel$, electron momentum parallel to the surface. The multielectron decay results in the spreading of the excitation energy among the substrate electrons. Thus, only the multielectron decay, Γ_{ee}, corresponds to a decay of the energy of the excited electron. However, in both decays, the excited electron(s) in the final state cannot be detected at the same place as the alkali resonance in a TR-2PPE spectrum, either because of the energy change or because of the large $k_\parallel$ of the electron. So, Γ_T, the decay rate of the quasistationary state should correspond to the decay rate observed in a TR-2PPE experiment. The situation would be different in the absence of a projected band gap. Then, the RCT decay populates states around $k_\parallel = 0$, which, apart from transport effects, can still be detected together with the quasistationary state in a TR-2PPE experiment. In that case, Γ_T does not correspond to the signal decay in a TR-2PPE experiment. Intuitively, if the adsorbate state is extremely short lived, there is no real trapping of the excited electron around the adsorbate and practically a TR-2PPE experiment looks at the Cu excited electron decay, which is governed by multielectron decay. Possibly, the situation could be different from that of a clean Cu surface, due to changes in the oscillator strengths, i.e., to changes in the distribution of intermediate Cu states in the 2PPE process.

III. RESULTS

A. One-electron decay (RCT)

Figure 1 presents the WPP results for the energy and the one-electron decay rate, Γ_{RCT} of the lowest level of the various alkalis in front of a Cu(111) surface. Although the adsorption corresponds to a well-defined alkali-Cu distance, the results are presented in a finite range of Z, around the typical adsorption heights Z_{ads}. The Z distances are measured from the Cu(111) image plane, which, for the model potential[33] used here, is located $2.2a_0$ from the last Cu plane. As the alkali-surface distance Z goes to infinity, these states correlate with the lowest-lying state of the alkali: $3s$, $4s$, $5s$, and $6s$ for Na, K, Rb, and Cs, respectively. The equilibrium ad-

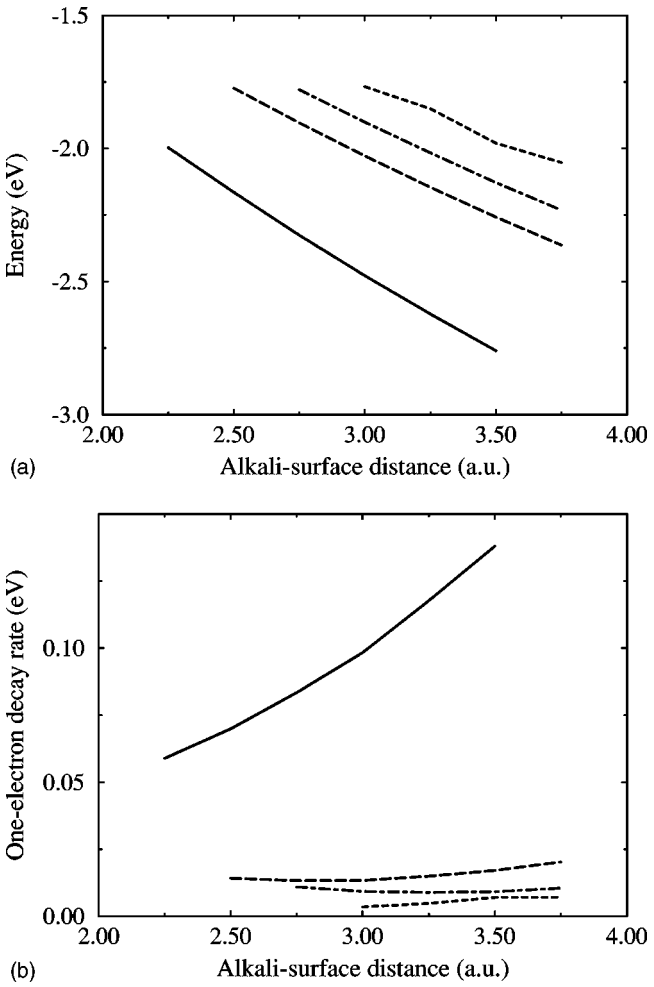

FIG. 1. (a) Energy of the lowest-lying excited state of the alkali/Cu(111) systems as a function of the alkali-surface distance. The distance is measured from the Cu(111) image reference plane and the level energy is given relative to the vacuum level. Na, full line; K, long dashed line; Rb, dashed-dotted line; Cs, short dashed line. (b) Same as (a), for Γ_{RCT}, the one-electron decay rate of the lowest-lying excited state of the alkali/Cu(111) systems.

sorption heights Z_{ads} for the various alkalis have been obtained from the literature. For Cs, $Z_{\mathrm{ads}}=3.5a_0$ was deduced from LEED experiments[43] or extracted from the coverage dependence of the surface work function.[44] For Rb, backscattering x-ray standing-wave measurements[45] yielded a value $Z_{\mathrm{ads}}=3.6a_0$. For K, Z_{ads} has been computed[46] to be $3.4a_0$. For Na, structure computations yielded an adsorption distance of $2.5a_0$ (Ref. 46) and in the $(2.4-2.6)a_0$ range;[47] these are consistent with a value of $2.3a_0$ extracted from the coverage dependence of the surface work function.[48] One can also stress here that for room-temperature experiments, the thermal population of the vibrational levels in the adsorption well results in a rather broad distribution of adsorption distances, leading to a significant broadening effect (see a discussion in Ref. 10 for the Cs and Na cases).

In Fig. 1(a), the energy of the various levels is seen to steadily increase when the alkali approaches the surface, this is a consequence of the image charge interaction that, in a simple first-order approach, would lead to a $1/(4Z)$ behavior

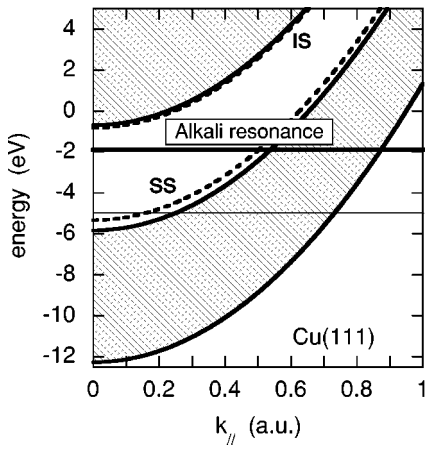

FIG. 2. Schematic picture of the electronic structure of the alkali/Cu(111) system as a function of $k_{\parallel}$, the electron momentum parallel to the surface. The gray area represents the 3D propagating bulk states. Thick dashed line: surface state (SS) and first image state (IS). Thin horizontal line: Fermi level. Thick horizontal line: typical energy position of the alkali resonance.

of the level energy. This feature is common to neutral atoms interacting with a metal surface and is not influenced by the peculiarities of the Cu(111) surface electronic structure. For the whole range of distances shown in Fig. 1, the adsorbate levels are degenerate with the Cu *L*-band gap.

In contrast to the level energy, the RCT decay rate Γ_{RCT} presented in Fig. 1(b) does exhibit a strong effect of the Cu(111) projected band gap; all the alkalis appear to be stabilized on the Cu(111) surface. On a free-electron metal surface, the one-electron decay rate of the alkalis are typically in the 1-eV range for typical alkali adsorption distances.[6–8] Here, on Cu(111), they are found to be between one and two orders of magnitude smaller. The very strong effect of the projected band gap found for Cs/Cu(111) is then also present for the other alkalis, although the absolute values of the decay rates differ from one alkali to the other. The one-electron decay rates Γ_{RCT} follow the order of the alkali size: Na, K, Rb, and Cs, the heavier being associated with the smallest width.

Let us briefly recall the interpretation of the blocking of the RCT on Cu(111) (see also in Refs. 11 and 12). Figure 2 presents a schematic view of the band structure of Cu(111), which illustrates the RCT blocking effect. The RCT process (transitions at constant energy) corresponds to the electron tunneling through the barrier separating the adsorbate and the substrate. It is hugely favored along the surface normal, where the transparency of the barrier is the highest. The projected band gap forbids tunneling along the surface normal and the RCT can only populate 3D propagating metal states with a minimum electron momentum parallel to the surface, $k_{\parallel,\mathrm{min}}^{\mathrm{3D}}$. Comparing this situation to that of the free-electron metal, would lead to the prediction of a drastic drop in the RCT decay rate. However, there exists a surface state on Cu(111) that can also be populated by the transient adsorbate state decay; in that case the final electron momentum parallel to the surface is $k_{\parallel}^{\mathrm{SS}}$. The surface state protrudes from the surface and can thus be very active in the RCT. The surface

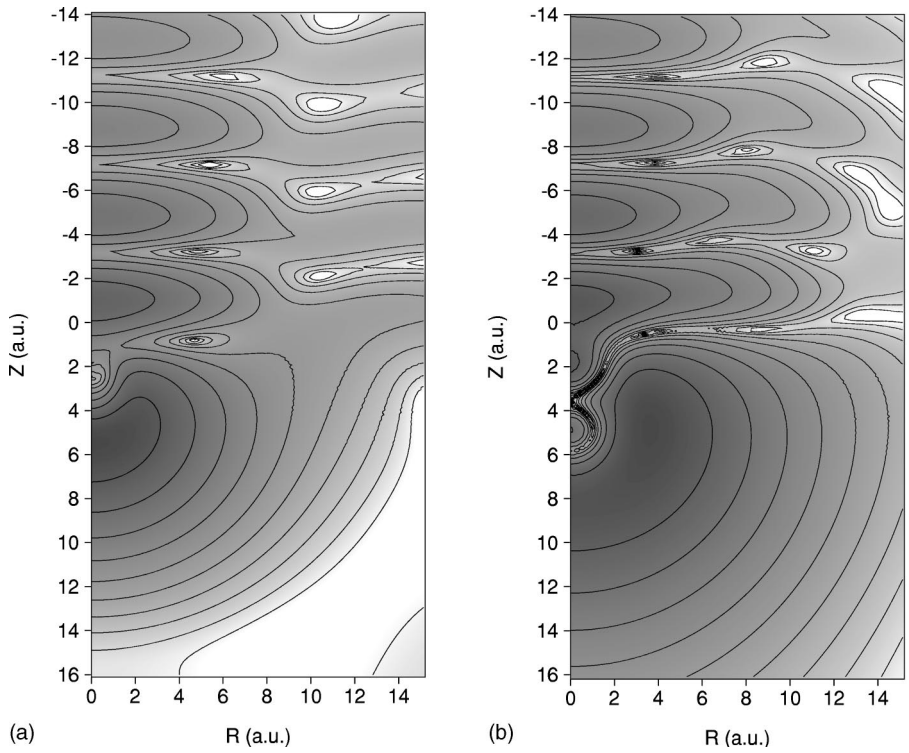

FIG. 3. (a) Contour plot of the resonant wave function Ψ_R in the Na/Cu(111) system. $\ln(|\Psi_R|)$ is presented in cylindrical coordinates parallel and perpendicular to the surface. z, the coordinate normal to the surface, is positive in vacuum and the image plane is located at $z=0$. The contour lines (thin full lines) correspond to 0.5 steps. The dark areas correspond to large probabilities of the presence of the electron. The Na center is located at $2.5a_0$ on the symmetry axis. (b) Contour plot of the resonant wave function Ψ_R in the Cs/Cu(111) system. $\ln(|\Psi_R|)$ is presented in cylindrical coordinates parallel and perpendicular to the surface. z, the coordinate normal to the surface, is positive in vacuum and the image plane is located at $z=0$. The contour lines (thin full lines) correspond to 0.5 steps. The dark areas correspond to large probabilities of presence of the electron. The Cs center is located at $z=3.5a_0$ on the symmetry axis.

state contribution can alter the above conclusion on the effect of the band gap on the RCT decay rate. As found for negative ions close to the Cu(111) surface or for Li atoms far from the surface,[11] the excited state decay towards the 2D surface state continuum can be faster than for a free-electron metal surface. In fact, it turns out that the polarization of the excited states localized on the alkali adsorbates plays a very important role in their stabilization. These transient excited states are polarized by their interaction with the surface, leading to a repulsion of the electronic cloud from the surface. This polarization of the adsorbate electronic cloud is illustrated in Fig. 3, which presents the wave packet corresponding to the quasistationary state in the Na and Cs cases. The image plane is located at $z=0$, and the metal extends to the upper part of the figure. One recognizes the strongly perturbed atomic wave function around the nucleus center and a continuum part corresponding to the decay of the quasistationary state into the metal; the latter is limited due to the scale choice of the figure. The oscillations visible inside the metal around the symmetry axis have the periodicity of the (111) planes in Cu; this wave extending into the metal is evanescent, as a consequence of the projected band gap (see the discussion in Ref. 21). In both the Na and Cs cases, one can see that the spherical symmetry of the electronic cloud around the alkali nucleus, which exists in the free atom, has disappeared. Due to the interaction with the metal, the resonant wave function is strongly repelled toward vacuum. This polarization effect, which is also present in the case of a free-electron metal, results in a decrease of the overlap between adsorbate and metal states and thus strongly enhances the band-gap effect. In addition, the polarization creates a node in the angular dependence of the resonant wave function. This nodal structure leads to cancellations in the adsorbate-metal states coupling terms. In fact, in the Cs case, it leads to a quasicancellation of the coupling with the surface state around the $k_{\parallel}^{SS}$ momentum and strongly attenuates this decay channel.

The adsorbate polarization thus strongly enhances the band-gap effect, this is clearly visible in the Z dependence of Γ_{RCT} for Cs/Cu(111) in a large Z range (see, e.g., Fig. 2 in Ref. 12), where Γ_{RCT} drops when the polarization sets in. The stabilization of the alkali states thus results from the combined effect of the band gap, of the surface state, and of the polarization of the atom.

B. Multielectron decay

The wave function Ψ_R contains the resonance wave function together with a continuum part associated with its decay by RCT (see, e.g., Fig. 3 and its discussion). The part of the wave function associated to this decay (outgoing wave leaving the adsorbate) should not be included in the multielectron

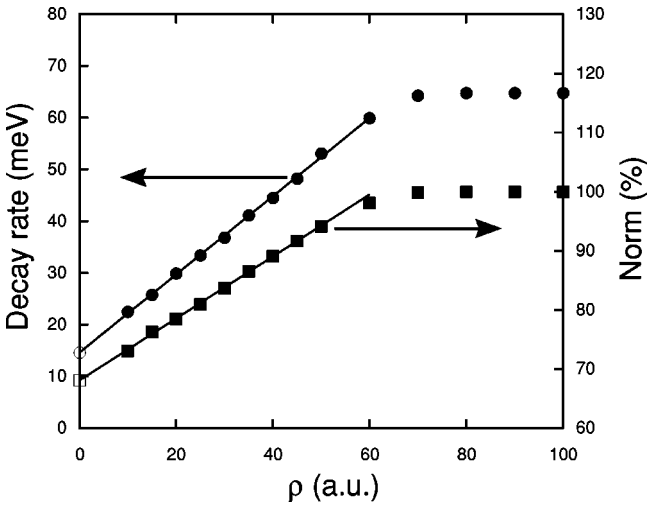

FIG. 4. Removal of the continuum part in the multielectron decay calculation. Black dots and left scale: multielectron decay rate computed with a truncated wave function as a function of the truncation radius ρ_{max} (see text). Black squares and right scale: norm of the truncated wave function as a function of the truncation radius ρ_{max} (see text).

decay rate calculation to avoid double counting. It corresponds to the situation where the excited-state decay has already occurred; even if the outgoing electron can afterwards be inelastically scattered by a Cu electron, this would not contribute to the excited-state decay as observed in a TR-2PPE experiment (see discussion in Sec. II C). The contribution from the RCT outgoing wave was removed from the calculation of Γ_{ee} by performing a set of calculations where the Ψ_R wave function was set to zero outside of a cylinder of radius $\rho=\rho_{max}$. Due to outgoing flux conservation, the continuum contribution in $\Gamma_{ee}(\rho_{max})$ varies linearly with ρ_{max}. In contrast, the resonant part is constant, as long as ρ_{max} is large enough to encompass the entire resonant wave function and small enough not to overlap the absorbing potential at the grid boundary. Extrapolation of $\Gamma_{ee}(\rho_{max})$ to small ρ_{max} thus yields the decay rate of the resonance. This extrapolation is illustrated in Fig. 4 for the case of Na, where we show Γ_{ee} and Q as functions of the cylinder radius ρ_{max}. Q is the norm of the Ψ_R wave function inside the cylinder of radius ρ_{max}. The absorbing potential at the grid boundary causes Ψ_R to go to zero beyond a certain radius and this accounts for the stabilization of Γ_{ee} and of Q at large ρ_{max}. Extrapolating the linear behavior of the wave function norm to $\rho_{max}=0$ yields Q_0, the fraction of Ψ_R that corresponds to the resonance wave function without the continuum contribution. The linear behavior of $\Gamma_{ee}(\rho_{max})$ extrapolated to $\rho_{max}=0$ and renormalized via Q_0 yields the multielectron decay rate of the resonance. It is shown in Table I for the various alkalis at their adsorption distance. Γ_{ee} is found to be only weakly dependent on Z, the adsorbate-substrate distance. In Fig. 4, it appears that Q_0 is significantly smaller than 1 in the Na case, showing the importance of the RCT decay in this case. The importance of this correction for the multielectron decay rate Γ_{ee} of the resonance varies with the alkali. It is more important for the lighter alkalis that exhibit a larger RCT decay rate and thus a larger outgoing wave component in the Ψ_R wave function. In the Cs case, removing the continuum contribution only amounts to a correction of around 15%.

C. Total decay rate

The present results for the various decay rates (one-electron, multielectron, and total) of the quasistationary states are summarized in Table I for the various alkalis. The results are given for the adsorbates located at their adsorption height and they are compared with TR-2PPE experimental results.[1–4,9] Quantitatively, the present Cs results are in between the two experimental results, the Rb results are in

TABLE I. Energy and decay rate of the first excited states of the alkali/Cu(111) systems.

	Na/Cu(111)	K/Cu(111)	Rb/Cu(111)	Cs/Cu(111)
		Present results		
Adsorption height (measured from image plane)	$2.5a_0$	$3.4a_0$	$3.6a_0$	$3.5a_0$
Energy (eV) (with respect to vacuum)	−2.17	−2.21	−2.17	−1.98
One-electron decay rate Γ_{RCT} (meV)	70	16	10	7
Inelastic electron-electron decay Γ_{ee} (meV)	22	18	17	15
Level lifetime $\tau=1/(\Gamma_{RCT}+\Gamma_{ee})$ (fs)	7	19	24	30
		Experiments		
Level lifetime (fs)	1.6 (300 K) (Ref. 9)		25 (33 K) (Ref. 9)	15±6 (300 K) (Refs. 1 and 2) 50 (33 K) (Refs. 3 and 9)

excellent agreement and the present Na lifetime is significantly larger than the experimental value. The present theoretical results exhibit the same variation as the experiments: the heavier the alkali is, the longer lived the excited state on Cu(111) is.

In the Cs case, the two experimental results are different; they were obtained in different experimental conditions, in particular, at different temperatures. Various effects can be invoked for this difference. First, the electron-phonon excitation could play a role in the excited-state decay. Indeed, the decay rate induced by the electron-phonon interaction varies at finite temperature as[49] $\Gamma_{e\text{-ph}}=2\pi\lambda k_B T$, where λ is the electron-phonon coupling constant. This coupling constant is not known in the present case. From the argument presented in the Introduction, it can be thought to be significantly smaller than the corresponding value for the Cu(111) surface state. So, we do not think that the electron-phonon contribution could dominate the state decay at room temperature, although including it would improve the agreement between the present calculations and experiments at room temperature. The second effect that can be invoked for the experimental differences is the role of the adsorbate motion induced by the electronic excitation. As discussed in Ref. 10, the adsorbate motion results, at low T, in a deeply modified time dependence of the signal in a TR-2PPE experiment, from which the excited-state lifetime cannot be extracted using the usual straightforward method, based on an exponential fit of the excited-state population decay.

IV. DISCUSSION

Table I shows that the difference of decay rates between the alkalis is larger for the RCT rate (a factor 10) than for the multielectron decay (factor 1.5). However, the relative order of the decay rates is the same for Γ_{RCT} and Γ_{ee}, the heavier alkalis having smaller decay rates. The difference between the various alkalis then appears to be mainly governed by Γ_{RCT}, which we discuss further below.

Different factors can be expected to influence the Γ_{RCT} decay rate and can thus be invoked to account for the different Γ_{RCT} rates of the various alkalis.[2,9,11,12,17] First of all, one can invoke an effect of the adsorption height. Indeed, the overlap between adsorbate localized and metallic states varies rapidly with the adsorbate-surface distance and one could expect this to be reflected in the Γ_{RCT} rates. This is the case for the free-electron metal surface (see, e.g., Ref. 8), where Γ_{RCT} increases rapidly as the alkali approaches the surface and saturates at small Z. The Z dependence of Γ_{RCT} on Cu(111) seen in Fig. 1 appears completely different from that in the free-electron case and does not follow the overlap argument, at least in the Z domain shown in the figure. In particular, in Fig. 1, the Z dependence of Γ_{RCT} for Na appears different from those of the other alkalis and is opposite to the above-mentioned overlap effect. This is attributed to the polarization effect. Na is less polarizable than the heavier alkalis and thus needs to be closer to the surface to fully experience the enhancement of the band-gap stabilization effect due to the polarization. The polarizabilities of Na, K, Rb, and Cs are equal to 24.08, 43.4, 47.3, and 59.6 Å, respectively.[50] The enhancement of the band-gap effect accounts for the drop of the Γ_{RCT} rate for Na as Z decreases. A similar drop of Γ_{RCT} when Z decreases also exists in the other alkalis, however it occurs at larger Z than for Na (see, e.g., Fig. 2 in Ref. 12 for Cs). It also appears in Fig. 1 that the relative order of magnitude of the different alkali decay rates is not varying much with Z, at least in the Z range of the figure, and so, one cannot invoke the difference of adsorption distances between the alkalis to explain the difference between the RCT decay rates.

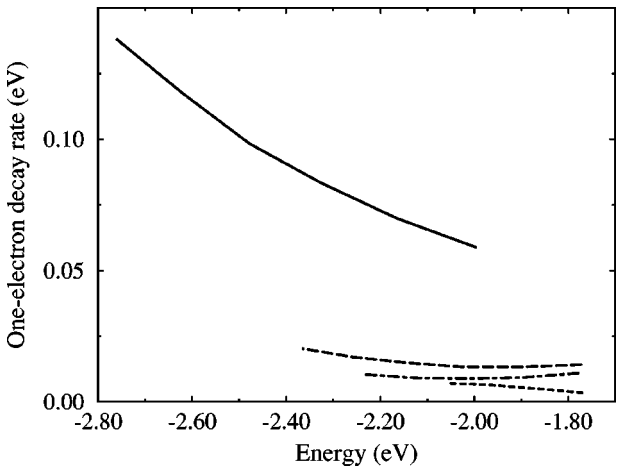

FIG. 5. One-electron decay rates Γ_{RCT} of the lowest-lying excited state of the alkali/Cu(111) systems as functions of the level energy. The level energy is given relative to the vacuum level. Na, full line; K, long dashed line; Rb, dashed-dotted line; Cs, short dashed line.

One could suspect the level energy to play a role in the difference between the alkali RCT rates. Indeed, the lower the level is in the projected band gap, the smaller $k_{\parallel,\min}^{3\mathrm{D}}$ and $k_{\parallel}^{\mathrm{SS}}$ are and the smaller one can expect the band-gap effect to be. This is the essence of the interpretation of the observed differences between the Cs/Cu(111) and Cs/Cu(100) cases[17] and it could also play a role here. However, one can first notice that, at the adsorption distance, the energies of the various alkali levels are very similar, they lie within 0.2 eV (see Table I). This is much smaller than the corresponding value in the free atoms (1.2 eV) and is partly a consequence of the different adsorption heights. Because of this energy similarity, the level energy cannot be a key parameter for explaining the width differences. To further test this point, we plotted the RCT decay rates as functions of the level energy in Fig. 5. The relative values of Γ_{RCT} for the different alkalis are not much modified as compared to Fig. 1(b), stressing that the level energy position is not the dominant reason for the width differences.

Since the band-gap stabilization effect is playing an important role in the absolute value of Γ_{RCT}, one should rather look for the origin of the differences in this effect. The atom polarization is very effective in enhancing the band-gap effect and indeed, one can notice that the relative order of magnitude of Γ_{RCT} for the alkalis follows the order of the atomic polarizabilities. The polarization aspect is quite visible in Fig. 3, where the electronic clouds are much distorted.

The wave packet in the Cs case extends further out into the vacuum than in the Na case. This is linked to the atomic polarizability of the two alkalis. Indeed, for a polarizable atom placed into a constant field, the displacement of the electron, measured as the mean value of the electron coordinate along the field, is proportional to the atomic polarizability. The different extensions of the wave packet into vacuum are then a direct consequence of the different atomic polarizabilities. The differences in the Γ_{RCT} rates for the various alkalis are then tentatively attributed to the different distortions of the electron wave packets, i.e., to the different polarizabilities of the alkali atoms.

As for the multielectron decay rate Γ_{ee}, it appears to be much less system dependent than Γ_{RCT}. Three factors can be thought to play a role. The first one is the phase space, e.g., the total number of final states accessible for the decay of the excited electron. This phase space is practically the same for all the alkalis we study because of the very similar excited-state energies at the adsorption distance. Therefore the phase-space factor does not lead to a system dependence of Γ_{ee}. The two other factors, the overlap of the excited-state wave function with both bulk and surface states of the substrate [see Eq. (7)] and the polarization, are combined and lead to a system dependence of Γ_{ee}. Na corresponds to the smallest polarization and its adsorption distance is significantly shorter than for the other alkalis, which leads to a larger overlap between the excited-state wave function and the substrate states and accounts for the larger value of Γ_{ee} for Na. The three other alkalis, K, Rb, and Cs, are located at nearly the same distance from the substrate. Due to the stronger polarizability of the Cs atom, the excited-state wave function in the Cs/Cu(111) system extends further into vacuum than in the K(Rb)/Cu(111) systems. The overlap between the excited-state wave function and the substrate states then decreases along the sequence K, Rb, Cs and this accounts for the system dependence of Γ_{ee} seen in Table I.

V. CONCLUDING SUMMARY

We have reported on a theoretical study of the lifetime of the lowest excited states of the alkali/Cu(111) systems, with an emphasis of the comparison between the various alkalis (Na, K, Rb, and Cs). This complements our earlier studies on the Cs/Cu systems, focusing on the differences between various Cu surfaces.[11,17] The case of a single adsorbate on the surface is investigated, representative of the low alkali coverage situation. It appears that in all cases the projected band gap of the Cu(111) surface strongly inhibits the one-electron decay of the excited state (resonant electron transfer to the bulk), leading to a partial stabilization of the excited states. The one-electron decay being strongly reduced, the multielectron contribution (inelastic scattering on the Cu bulk electrons) can play a significant role. The decay rates via these two processes have been evaluated by a joint wave-packet propagation and many-body metal response approach.

The present results allow a discussion of the origin of the differences between the various alkali/Cu(111) systems. The theoretical lifetimes of the excited states are found to increase along the sequence Na, K, Rb, Cs, in agreement with the experimental TR-2PPE results.[1–3,9] This evolution along the alkali series is governed by the one-electron decay rate; the multielectron decay rate follows the same variation, although with a much smaller amplitude. In both cases, the differences between the different alkalis are tentatively attributed to the differences between the alkali atom polarizabilities. In front of a metal surface, the polarized excited electronic cloud is repelled from the surface leading to an enhancement of the projected band-gap effect (inhibition of the one-electron decay) and to a decrease of the overlap between the excited-state wave function and the Cu states (decrease of the multielectron decay rate): the larger the polarization effect is, the smaller the lifetime is.

ACKNOWLEDGMENTS

Stimulating discussions with A. K. Kazansky are gratefully acknowledged. This work was partially supported by the University of the Basque Country and the Basque Hezkuntza.

[1] M. Bauer, S. Pawlik, and M. Aeschlimann, Phys. Rev. B **55**, 10 040 (1997).
[2] M. Bauer, S. Pawlik, and M. Aeschlimann, Phys. Rev. B **60**, 5016 (1999).
[3] S. Ogawa, H. Nagano, and H. Petek, Phys. Rev. Lett. **82**, 1931 (1999).
[4] H. Petek, M. J. Weida, H. Nagano, and S. Ogawa, Science **288**, 1402 (2000).
[5] H. Guo, P. Saalfranck, and T. Seideman, Prog. Surf. Sci. **62**, 239 (1999).
[6] N. D. Lang and A. R. Williams, Phys. Rev. B **18**, 616 (1978).
[7] P. Nordlander and J. C. Tully, Phys. Rev. B **42**, 5564 (1990).
[8] A. G. Borisov, D. Teillet-Billy, J. P. Gauyacq, H. Winter, and G. Dierkes, Phys. Rev. B **54**, 17 166 (1996).
[9] H. Petek, H. Nagano, M. J. Weida, and S. Ogawa, J. Phys. Chem (to be published).
[10] A. G. Borisov, A. K. Kazansky, and J. P. Gauyacq, Phys. Rev. B **64**, 201105 (2001).
[11] A. G. Borisov, A. K. Kazansky, and J. P. Gauyacq, Surf. Sci. **430**, 165 (1999).
[12] J. P. Gauyacq, A. G. Borisov, G. Raseev, and A. K. Kazansky, Faraday Discuss. **117**, 15 (2000).
[13] M. C. Desjonquères and D. Spanjaard, *Concepts in Surface Science*, Surface Science Vol. 40 (Springer-Verlag, Berlin, 1993).
[14] P. M. Echenique and J. B. Pendry, J. Phys. C **11**, 2065 (1978).
[15] P. M. Echenique and J. B. Pendry, Prog. Surf. Sci. **32**, 111 (1990).
[16] E. V. Chulkov, I. Sarria, V. M. Silkin, J. M. Pitarke, and P. M. Echenique, Phys. Rev. Lett. **80**, 4947 (1998).

[17] A. G. Borisov, J. P. Gauyacq, A. K. Kazansky, E. V. Chulkov, V. M. Silkin, and P. M. Echenique, Phys. Rev. Lett. **86**, 488 (2001).
[18] A. Eiguren, B. Hellsing, F. Reinert, G. Nicolay, E. V. Chulkov, V. M. Silkin, S. Hüfner, and P. M. Echenique, Phys. Rev. Lett. **88**, 066805 (2002); (to be published).
[19] J. J. C. Geerlings and J. Los, Phys. Rep. **190**, 133 (1990).
[20] A. G. Borisov, A. K. Kazansky, and J. P. Gauyacq, Phys. Rev. Lett. **80**, 1996 (1998).
[21] A. G. Borisov, A. K. Kazansky, and J. P. Gauyacq, Phys. Rev. B **59**, 10 935 (1999).
[22] L. Guillemot and V. Esaulov, Phys. Rev. Lett. **82**, 4552 (1999).
[23] T. Hecht, H. Winter, A. G. Borisov, J. P. Gauyacq, and A. K. Kazansky, Phys. Rev. Lett. **84**, 2517 (2000).
[24] L. Bartels, G. Meyer, K.-H. Rieder, D. Velic, E. Knoesel, A. Hotzel, M. Wolf, and G. Ertl, Phys. Rev. Lett. **80**, 2004 (1998).
[25] E. Knoesel, T. Hertel, M. Wolf, and G. Ertl, Chem. Phys. Lett. **240**, 409 (1995).
[26] M. Wolf, A. Hotzel, E. Knoesel, and D. Velic, Phys. Rev. B **59**, 5926 (1999).
[27] J. P. Gauyacq, A. G. Borisov, and G. Raseev, Surf. Sci. **490**, 99 (2001).
[28] N. Lorente and M. Persson, Faraday Discuss. **117**, 277 (2000).
[29] A. G. Borisov, J. P. Gauyacq, and S. V. Shabanov, Surf. Sci. **487**, 243 (2001).
[30] J. N. Bardsley, Case Stud. At. Phys. **4**, 299 (1974).
[31] L. Kleinman and D. M. Bylander, Phys. Rev. Lett. **48**, 1425 (1982).
[32] J. R. Chelikowsky, N. Troullier, and Y. Saad, Phys. Rev. Lett. **72**, 1240 (1994).
[33] E. V. Chulkov, V. M. Silkin, and P. M. Echenique, Surf. Sci. **391**, L1217 (1997); **437**, 330 (1999).
[34] M. D. Fleit and J. A. Fleck, J. Chem. Phys. **78**, 301 (1982).
[35] R. Kosloff, J. Phys. Chem. **92**, 2087 (1988).
[36] R. Kosloff and D. Kosloff, J. Comput. Phys. **63**, 363 (1986).
[37] G. Jolicard, C. Leforestier, and E. J. Austin, J. Chem. Phys. **88**, 1026 (1988).
[38] D. Neuhauser and M. Baer, J. Chem. Phys. **91**, 4651 (1989).
[39] P. M. Echenique, J. M. Pitarke, E. V. Chulkov, and A. Rubio, Chem. Phys. **251**, 1 (2000).
[40] L. Hedin and S. Lundqvist, Solid State Phys. **23**, 1 (1969).
[41] E. V. Chulkov, V. M. Silkin, and M. Machado, Surf. Sci. **482**, 693 (2001).
[42] M. A. Van Hove, W. H. Weinberg, and C. M. Chan, *Low Energy Electron Diffraction* (Springer-Verlag, Berlin, 1986).
[43] S. A. Lindgren and L. Wallden, Phys. Rev. B **28**, 6707 (1983).
[44] S. A. Lindgren and L. Wallden, Solid State Commun. **25**, 13 (1978).
[45] X. Shi, C. Su, D. Heskett, L. Berman, C. C. Kao, and M. J. Bedzyk, Phys. Rev. B **49**, 14 638 (1994).
[46] L. Padilla-Campos, A. Toro-Labbé, and J. Maruani, Surf. Sci. **325**, 24 (1997).
[47] J. M. Carlsson and B. Hellsing, Phys. Rev. B **61**, 13 973 (2000).
[48] X. Y. Wang, R. Paiella, and R. M. Osgood, Jr., Phys. Rev. B **51**, 17 035 (1995).
[49] G. Grimvall, in *The Electron-Phonon Interaction in Metals*, edited by E. Wohlfarth, Selected Topics in Solid State Physics (North-Holland, New York, 1981).
[50] *CRC Handbook of Chemistry and Physics*, edited by R. C. Weast (CRC, Boca Raton, FL, 1996).